Solid Freeform Fabrication 2022: Proceedings of the 33rd Annual International Solid Freeform Fabrication Symposium – An Additive Manufacturing Conference
Reviewed Paper

LIGHTWEIGHT ADDITIVELY MANUFACTURED BELL CRANK

Carlos Rodriguez[1 2], Sol Barraza[1 2], Julio Diaz[1 2], Edel Arrieta[1 2], Alejandro Hernandez[1 2], Adam Hicks[2], Ryan B. Wicker[1 2], and Francisco Medina[1 2]

[1] Department of Aerospace and Mechanical Engineering, University of Texas at El Paso, El Paso, TX, 79968, USA

[2] W.M. Keck Center for 3D Innovation

[3] Air Force Research Laboratory, WPAFB, OH, 45433, USA

Abstract

Due to the long service life of Air Force Legacy aircrafts, some companies that used to manufacture their components and spares are no longer able to do so. In this case, Additive Manufacturing (AM) poses as a viable option to manufacture those spares when needed and even improve their cost, weight, and performance. This project focuses on designing, building and testing of a bell crank, a largely needed spare part in these aircrafts, in order to achieve weight reduction and increased strength. The designing process was done using Fusion 360's Generative Design, which can be tailored to produce different outcomes which satisfy the user's needs. Fused Deposition Modeling (FDM) was chosen for the manufacturing method with ABS chosen as the testing material. The components were tested using an adapted Instron 5900 Series. The initial testing phase served to show that a horizontal build proved to be the most optimal out of three orientations tested, while the second phase showed that the Bk_fpx design, which focused on strength, was the best performing due to its strength-to-weight ratio (29.7) and cost ($160). It is recommended that all this work is continued by the metal AM method laser powder bed fusion (LPBF) with companies such as Selective Laser Melting (SLM) using Aluminum since this method is capable of rapid prototyping and this material would help minimize the weight in the aircraft.

Introduction

This project focused on posing AM as a manufacturing method for Out-of-Production Spares (OOPS). An Air Force legacy aircraft has an average service life of about 27 years, and in extreme cases can get up to 70 years[1]. For this reason, it can be difficult to find spare parts for them as original manufacturers may stop supporting them in the time that they are in service[2].

For the low volume of the parts (in demand), manufacturing these spare parts by traditional means is not the most efficient, as such methods can cause a lot of waste and are mainly time effective only when used in mas production. AM poses as a solution for that drawback as it can build unique and complex parts at a reduced lead time, material waste and base cost[3]. AM provides the opportunity to innovate on previous designs as it also possess the capability to build multiple complex geometries with a variety of lightweight materials [4].

The objective of this project is to design, build, and test a bell crank focusing on utilizing AM capabilities and techniques. A bell crank is a pivoting mechanism that allows for the change

of motion of the air craft at varying angles and is primarily needed as a form of mechanical movement within the aircraft. The bell crank is also a highly requested item in terms of replacement parts[5]. The design objective was to maximize the strength to weight ratio and minimize the cost and manufacturing lead time; this while meeting baseline mechanical properties of a traditionally manufactured part.

Initial Constraints

The team was provided a set of constraints and loading directions, without specification of the actual loadings, to guide the bell crank design illustrated below. The newly designed part was required to meet the same hole patterns and physical boundaries as the original part. The constraints consisted of an obstacle block and the 4 bell crank pins: a driver, pivot, and two follow pin. The design would have to connect these pins for movement and avoid colliding with the obstacle geometry. At the same time, it should be the strongest and lightest we can devise it to be.

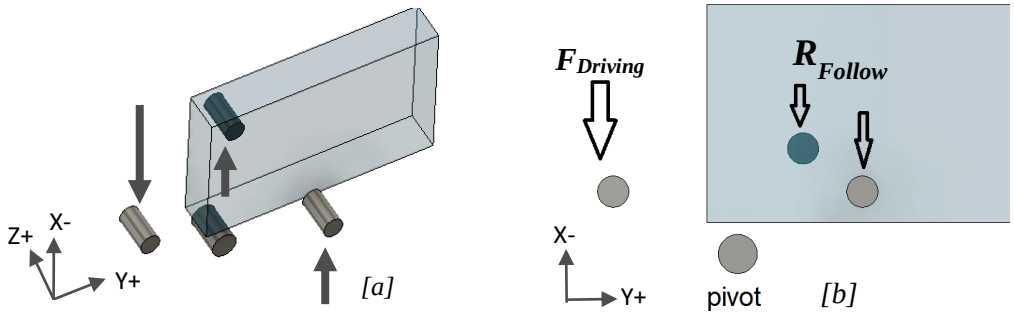

Figure 1: *Bell Crank Design Constraints isometric[a] and side[b](clear arrows are used to label forces).*

Procedure

Bell Crank Finite Element Analysis (FEA)

The design approach would consist of making design choices from results obtained through the Fusion 360 software. Following the original design constraints, an initial block design was made that connected the pins in a driver-pivot-follow fashion (Figure 2). This design intended to serve as a basis for an initial FEA analysis which would mimic the loading conditions the bell crank would be required to perform under. This would provide an expected loading force distribution that would serve as a guide for the initial design.

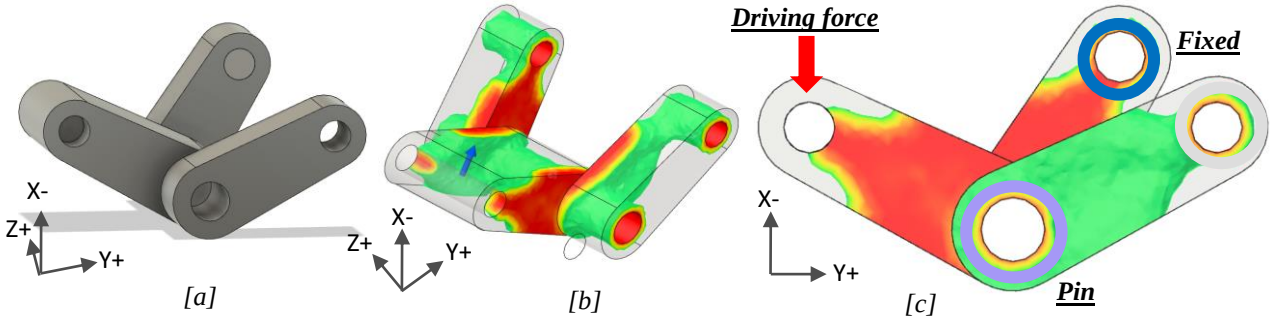

Figure 2: *Base design [a] with stress FEA [b] and stress FEA with labeled loading conditions [c]*

The FEA analysis was performed on the Autodesk Fusion 360 Simulation tab, which was the main CAD software used throughout this project. An arbitrary load was applied for the study to gain insight about the stress distribution which is necessary to create starting design shapes. The load was applied down on the driver pin, emulating the motion driving force with the follow pins fixed, having the pivot constrained as a rotating pin (Figure 2). The results indicated that the max stress would occur at the pivot, followed by the two follow connecting legs.

Initial Design

A new design was made from taking into consideration the results from the load path FEA. It connected the pins in an organic way that was meant to reduce the weight and utilize AM's ability to manufacture complex geometries. The design (as shown in Figure 3 below) connects the driving pin to the pivot (where it is reinforced), and then branches out to the two follow pins. The $\frac{1}{4}$" pins are surrounded by an $\frac{1}{8}$" ring with smooth connections to the pivot pin. These connections were designed observing the clearance of the obstacle block needed for movement.

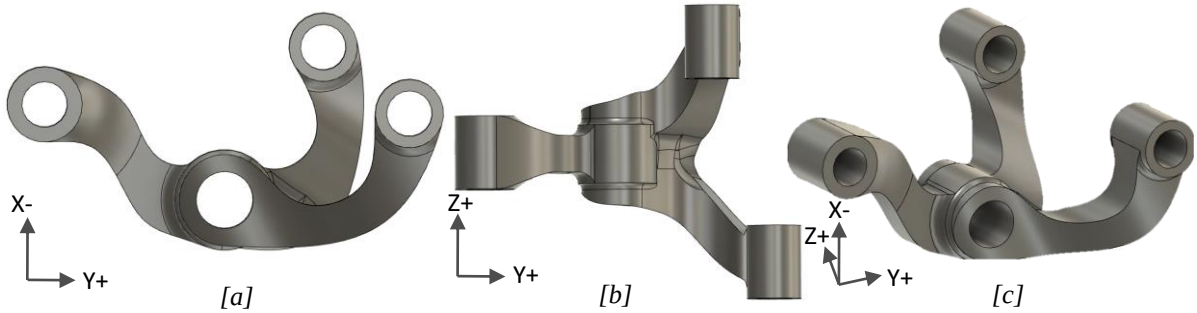

Figure 3: *Initial bell crank design with side [a], bottom [b], and isometric [c] view*

This design was then placed in another FEA analysis to record the expected strength for the bell crank using the same constraints and loading conditions from before. The FEA results indicated no concerning issues at the set load with a maximum displacement of 1.4 mm on the driving arm as seen on Figure 4. However, this design still did not provide a good distribution of stress through the part, as it still concentrated most of the stress onto one area. Ideally, we are looking for an even distribution of stress throughout the part which would lead to a failure on multiple areas. This would prevent catastrophic failure at maximum conditions and would ensure stronger parts.

Figure 4: *FEA with maximum displacement*

Generative Design

In addition to traditional forms of design, Fusion 360's Generative Design tool was used to further optimize the bell crank for weight reduction. This software function would provide feasible design options that can potentially be better than the team's initial design since the software would do all calculations and go through numerous iterations before providing the viable options. The generative design study requires an input of a combination of shape constraints and loading conditions in order to generate a suitable design solution[6].

Set Up

The shape constraints consist of the establishing of some key geometries such as the preserve geometries, obstacle geometries and a starting shape*. Preserve geometries (green highlighted shapes in Figure 5 below) are the CAD bodies that must remain in the final design; in this case: 1/8" rings around the pins. The obstacle geometries (marked in red) are areas where material cannot be added to; in this case: provided conditions, obstacle block, and pin cylinders. The obstacle block was broadened to account for rotation.

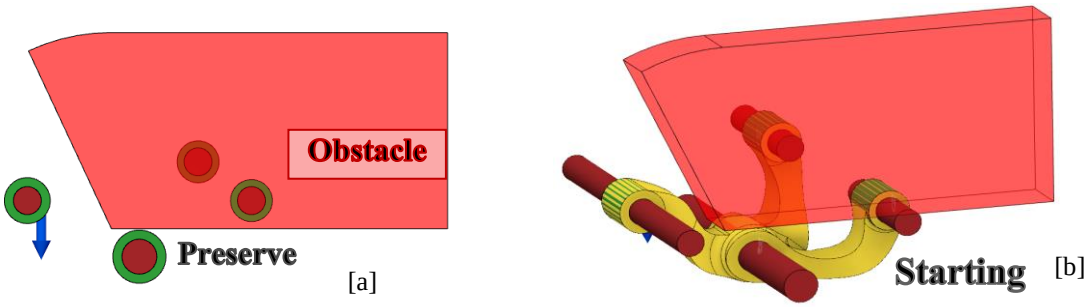

Figure 5: *GD shape constraints without [a] and with a starting shape [b]*

The starting shape (marked in yellow above) is any initial body for the software to base its optimization with. A starting shape is not always used; however it was needed for this study given that the obstacle geometry is in between two preserve bodies to guide the correct path and connections. For this study three starting figures were utilized: the initial design, a block, and skeleton shape. These starting geometries, shown in Figure 6 below, were chosen to study the effect of the starting shape on the design approach. The block starting shape was meant to give the software

excess material for it to take liberties of creating connections that focused on strength. The Skeleton starting shape is meant for allowed freedom of connections and meant to yield the most lightweight options. The generative design study also used the initial design as a starting shape to explore the possible optimizations on the current design.

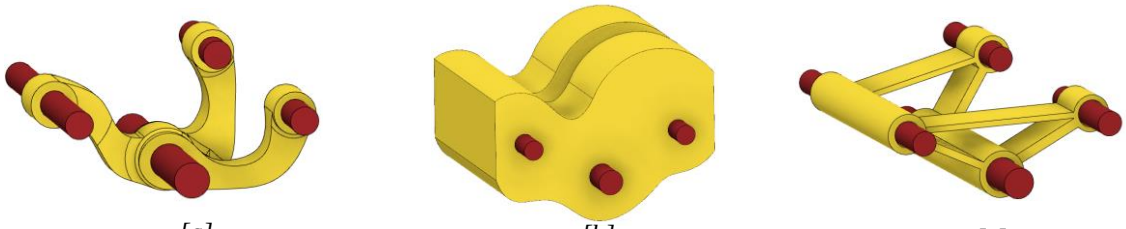

[a] *[b]* *[c]*

Figure 6: *Initial [a], Block [b] and Skeleton[c] Starting Shapes to optimize*

Following the geometrical constraints are the loading conditions. These conditions, much like the FEA loading conditions, instruct the software what forces the part is intended to withstand. Two loading condition variations (illustrated in Figure 8 below) were considered; one with a driving force on two fixed follows and the other with reaction forces and were ran with 100 lbf (450 N) and 250 lbf (1100 N) as driving force in order to get results that would focus on weight reduction (100 lbf) and strength (250 lbf). An arbitrary safety factor of 2 was also considered for both cases. A more concrete factor of safety, although not given in this case, would be accounted for and based off standards given by the Air Force.

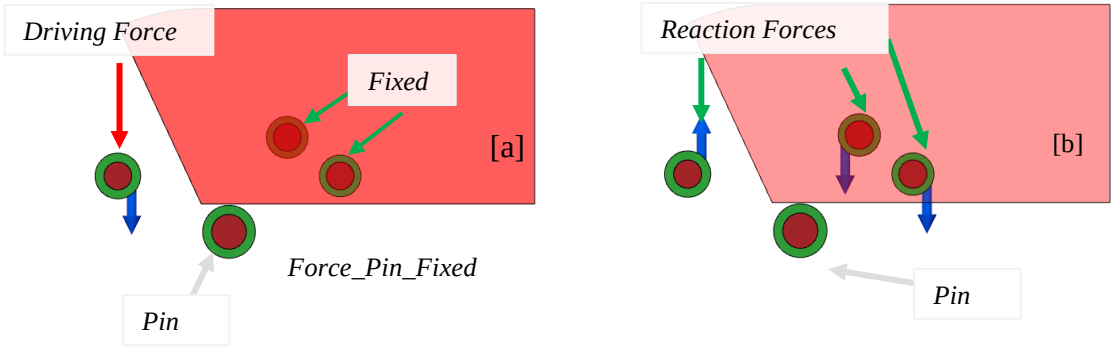

Figure 7: *Loading conditions schematic with fixed conditions [a] and with reaction forces [b]*

Table 1: Base Design Shapes and Load Case Models

Base Design Shapes and Load Case Models				
Starting Shape	**Load Case**			
	Force_Pin_Fix		***Force_Pin_Force***	
Skeleton	sk_fpx_100	sk_fpx_250	sk_fpf_100	sk_fpf_250
Block	k_fpx_100	bk_fpx_250	bk_fpf_100	bk_fpf_250
Current	c_fpx_100	c_fpx_250	c_fpf_100	c_fpf_250

After these parameters are set, a study is uploaded to the Autodesk Cloud to converge results. Then the software releases multiple design outcomes (show in Figure 8 below) for the user to select the most compatible one that fit their desired purposes. Once the outcomes were selected, they were converged to a CAD part and went through a manual editing phase. This design goes through a post processing polishing to allow for use and manufacture by smoothing out any features that could be improved upon or any flaw that a computer could detect. This includes expanding the clearance on the obstacle geometry for motion and reinforcing the pin joints and smoothing out any sharpness in their connections to each other.

Outcomes

Figure 8 below shows the bills of the parts selected at the left and a snapshot of the other converged designs to the right. These designs were chosen to test different design approaches; both C_fpf models were designed based on the initial design starting shape, under the loading condition force_pin_force. Version 1 C_fpf_v1 focused on robustness and maximizing strength, while version 2 C_fpf_v2 focused on weight reduction of the part. The third design, Bk_fpx, was based on the block starting shape and was under the force_pin_fixed loading condition. This outcome was chosen primarily from the difference in its design configuration. All designs had the same preserve and obstacle geometries and complied with a minimum safety factor of 2.

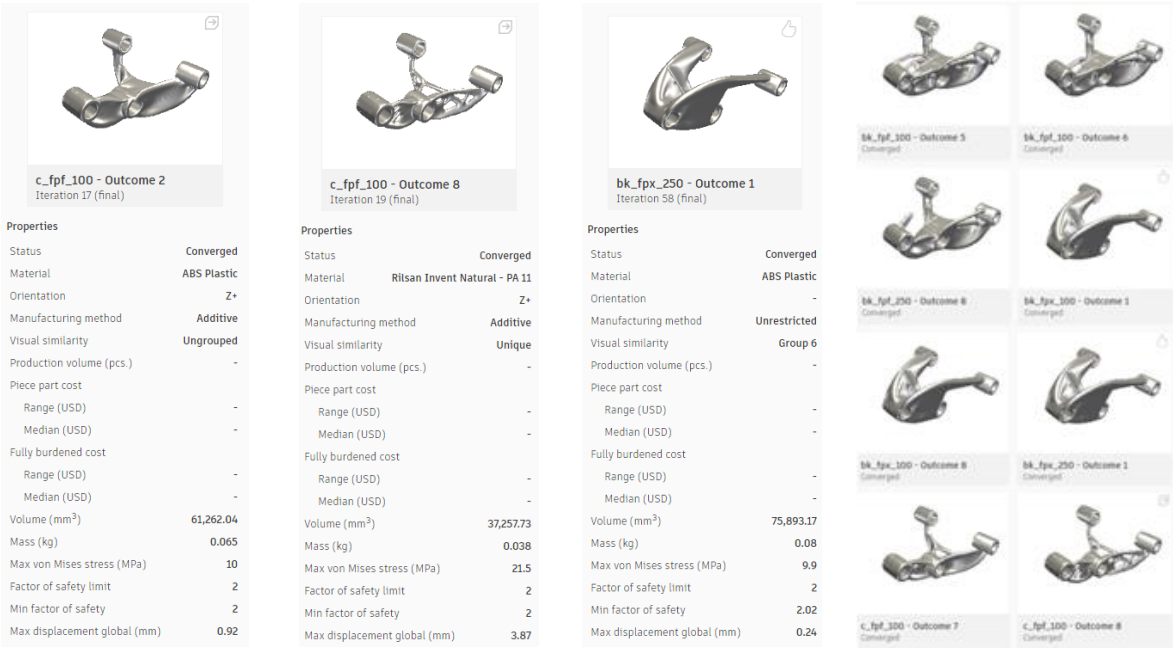

[a] *[b]* *[c]* *[d]*

Figure 8: *Generative Design Choices of the two C_fpf_100 and bk_fpx_250 outcomes [a], [b], and [c] respectively, with assortment of other converged designs [d]*

A FEA was performed on the three different designs. The same exact constraints and loads were used as for the past designs. The results expressed the following:

The FEA pointed out that the highest stress concentration would occur at the same place (Figure 9), the bottom area of where the pin holder passes through for both C_fpf_v1 and C_fpf_v2.

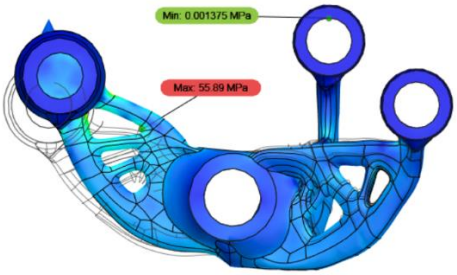

***Figure 9**: C_fpf_v2 model FEA*

Bk_fpx: Stress concentrations were minimal at the specified loading condition; however, these areas were not located on the driving arm (as the last designs). But on one of the other arms of the bell crank and at the bottom on where the main pin passes through (Figure 10).

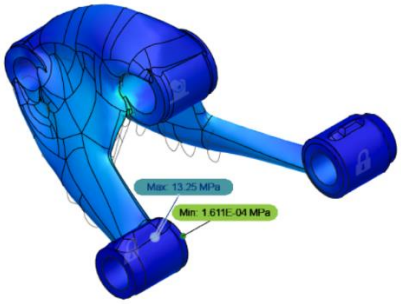

***Figure 10:** Bk_fpx model FEA*

Loading Conditions and Design Approach

Closer inspection of the design outcomes showed that Force_Pin_Fixed (fpx) led to an over-pivot approach (sequentially connecting the pivot, the driver and then the follow pins), while Force_Pin_Force (fpf) condition yielded a center-pivot design (pin connected to driver and follow without these two connecting to themselves). None of the outcomes based off the skeleton starting shape were used for testing because they did not converge with fit characteristics meant for the intended additive manufacturing technology such as orientation, mechanical properties, and other incompatibility issues. However, these outcomes showcased how the approach changed with loading conditions as shown below. This observation proved consistent across the results.

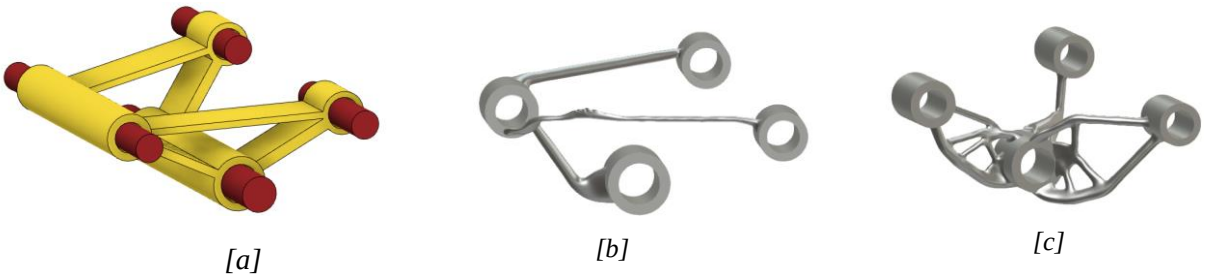

[a] *[b]* *[c]*

***Figure 11:** Skeleton starting shape [a] with sk_fpx_250 over-pivot [b] and center-pivot [c] optimization outcomes*

Manufacturing: Print set ups

FDM was chosen as the method of manufacturing. For this type of technology orientation and support structures should be considered as key. Other factors acknowledged were the cost, manufacturing time, material, repeatability, and quality[7].

Since orientation is a key factor in FDM, the part's layer-by-layer adhesion mechanical properties vary depending on the build orientation of a part[8]. This along with percentage of infill material and airgaps in between layer and extrusion lines affect the ultimate strength of the part[9]. Different orientations would be tested to determine an optimal orientation for the required performance and would be performed first to reduce the number of samples manufactured and tested.

Ultimately three of the more commonly used orientations were used, labeled as horizontal, vertical, and 45-degree angle shown (Figure 12) below. Other orientations were not utilized due to unsupported justification to do so and possible similar layer behavior to the ones selected. The three orientations were printed with default settings from the Stratasys CAD (Computer Aided Design) processing software, GrabCAD, with the only variance being the infill density set (100%). For all the designs the Stratasys F370 model was used, with ABS (Acrylonitrile Butadiene Styrene) as the material of choice, and GrabCAD as the main software to process the CAD files.

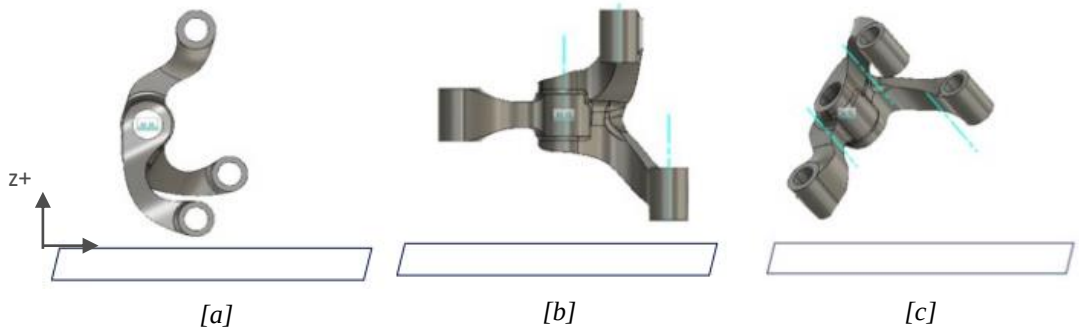

Figure 12: *Horizontal [a], vertical [b], and 45° [c] print orientations of model*

Table 2: Testing Parameters

Testing Parameters
Slicing height of 0.01 in.
Tips 14 for model and support
100% infill density
0.04 body thickness
Infill angle of 45-degree
Self-supporting angle of more than 43-degrees

ABS was chosen as the print material due to its availability, relatively low cost, and sturdy mechanical properties[10]. It is also known for being one of the materials with the highest print success rate on Stratasys machines.

For statistical purposes three samples of each geometry iteration were printed, resulting in a total of nine samples. Material cost, times and material used were provided by the in-house 3D printing services of the W.M. Keck Center for 3D Innovation which went as followed:

Table 3: FDM Build Descriptions

FDM Optimized Builds			
Design	**C_fpf_v1**	**C_fpf_v2**	**Bk_fpx**
Time	5h 49m	4h 35m	5h 15m
Model Material (in^3)	3.658	2.794	4.49
Support Material (in^3)	4.967	1.911	2.393
Manufacturing Cost ($)	$183	$141	$160

A preview of the build displays the model material in green (ABS) and the F123 QSR soluble support material in yellow. At the side of each sample there is a wipe tower which is used to purge excess material on the tips to avoid print failures, this is automatically done on this Stratasys machine.

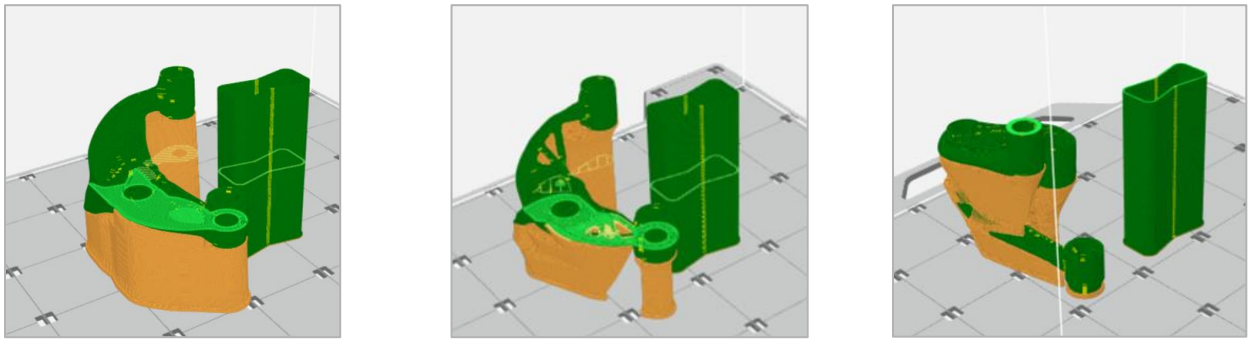

[a] *[b]* *[c]*

Figure 13: *Print Process Interface of C_fpf_v1 [a] C_fpf_v2 [b], and BK_fpx [c] models*

Manufacturing: Testing Fixture

An Instron 5900 Series was used for testing and the fixtures for a three-point bending test were adapted to accommodate for the different designs. The fixture was designed so that it was simpler to machine and could be adapted as needed case by case. For this reason, a plate was cut so that it can have 4 slots on one side and 2 slots on the other where the pin holders and the stoppers are going to be, respectively. The pin will let the bell crank rotate and the stopper will simulate the reaction forces the bell crank would encounter in a real scenario.

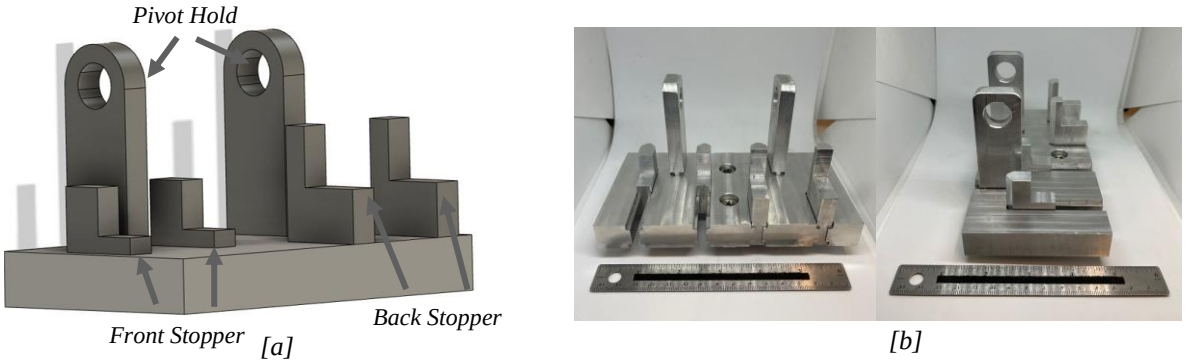

Figure 14: *Test fixture CAD [a] and physical apparatus [b]*

Components of Machined Fixture

Base with slots: Will hold together all the components, its slots make it easier to adapt for different type of bell cranks.

Stoppers: Inserted on the base and its main function is to provide a reaction force on the other two arms of the bell crank.

Pin holders: Its main function is to keep in place the main pin, it would also be inserted on the base through its slot.

Pins: Four pins are needed for this fixture, three of them would be of the same diameter but main one will not. Its main function is to either provide contact with the stoppers or to transfer the force from the top grip to the bell crank.

Test Procedure

The machine was set up with a maximum load of 10 kN where just the upper mount was pulling at a rate of 2 millimeters per minute and the bottom mount remained static. All the samples were tested under the exact same conditions and the Instron would be recalibrated whenever an offset bigger than 0.2 N was exhibited at no load conditions post testing. Prior to the test, the bell crack samples were marked with red tint in the areas where the FEA analysis predicted failure with the intention of comparing computed versus real failure.

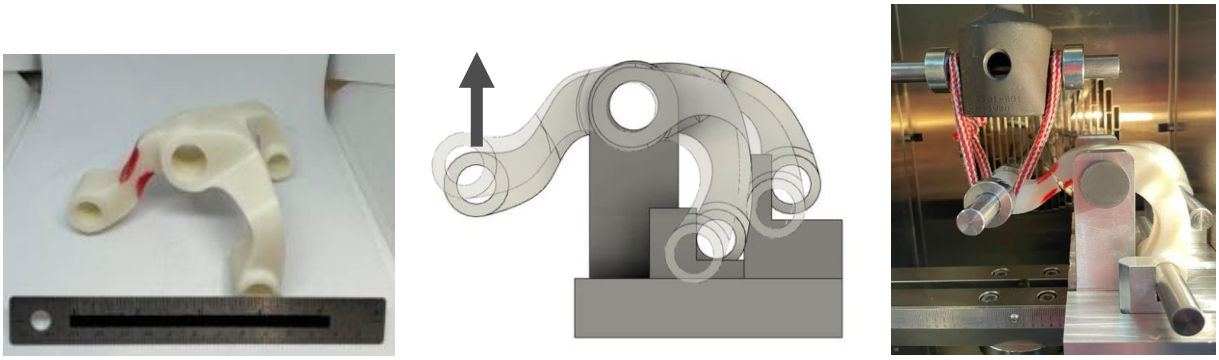

[a] *[b]* *[c]*

Figure 15: *Test set-up of a marked sample [a], expected movement [b], and Installed test [c]*

Table 4: Testing Procedure

Testing Procedure
1.Attach three-point bending bottom fixture to the Instron.
2.Attach pin to top grip.
3.Secure machined fixture on three-point bending bottom fixture.
4.Calibrate Instron.
5.Mount sample (3D printed bell crank) on the machined fixture.
6.Secure ropes from top grip to the pin on the bell crank's driving arm
7.Start test.

Orientation Results

When the different printing orientation samples were tested, it was concluded that the optimal orientation was building parts horizontally. Meaning that while performing the test each layer would be under tension, the forces would go along each layer instead of going across layers. Running this test identified the optimal printing direction that carried into the experiments that followed. Test data and results are illustrated in the figure below.

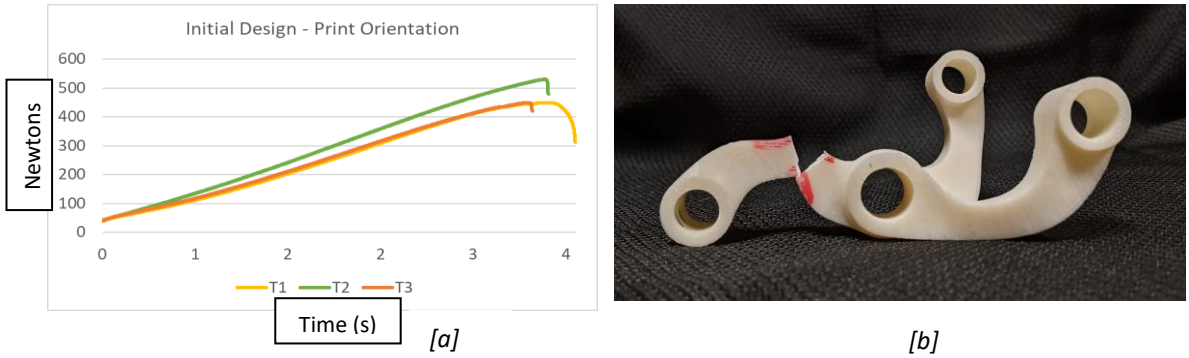

[a] *[b]*

Figure 16: *Orientation Test results [a] and fractures [b]*

Failure in these tests occurred in areas that were consistent with where the FEA analysis had predicted failure. The fracture surfaces, results tabulated below, provide insight into the expected mechanical failure in AM parts. The parts with the lowest UTS were parts that experienced a layer delamination failure, a failure type common among AM parts[11].

Table 5: Orientation Fracture Results

Orientation Fracture Tests			
Test	1	2	3
Direction	Vertical	Horizontal	45 Degrees
Ultimate Strength	448.9 N	529 N	448.8 N
Fracture Type	Layer delamination	Layer delamination	Cross layer
Fracture	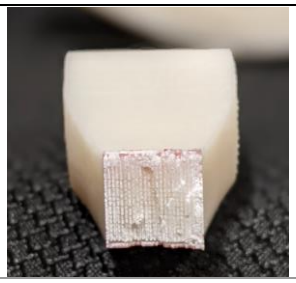	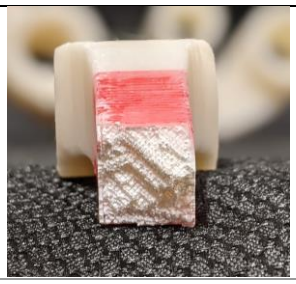	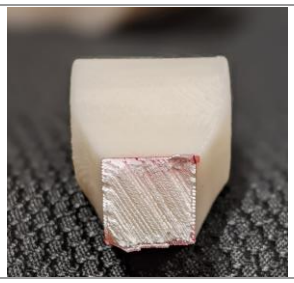

Once the orientation testing was complete, the geometry tests were run. Three samples of each design were printed, marked, and tested. Note: due to the variance in approach of the block-based design, some of the printed material had to be shaved off for it to fit in testing fixture.

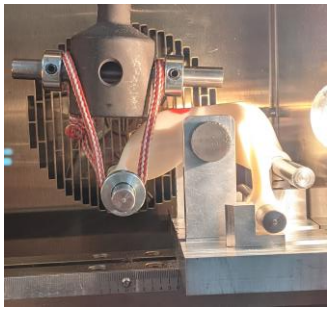

[a]

[b]

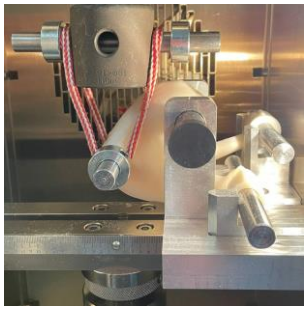

[c]

Figure 17: *Geometry Test Set-up of C_fpf version 1 [a], C_fpf version 2[b] and Bk_fpx [c] builds*

Design Results

C_fpf_v1 showed two points of failure (multiple points of failure are preferred as it indicates that not one point was significantly weaker than another). However, the points of failure were not where the FEA predicted, but rather over the pivot and at the follows. The test is surmised in the figure 18 below.

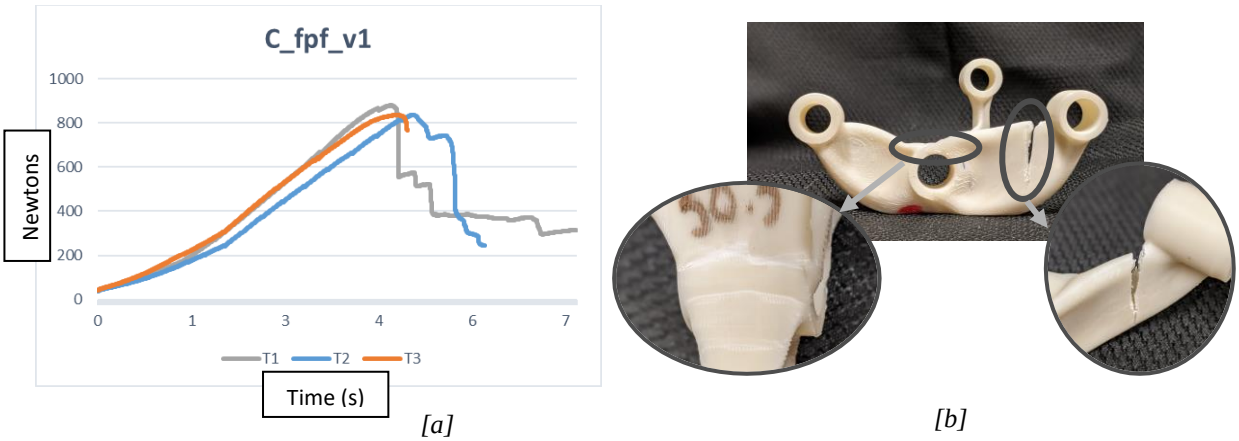

Figure 18: *C_fpf_v1 results [a] and fractures [b]*

C_fpf_v2 focused on weight reduction and was the design with the lowest Ultimate force, failing at an average of 200 N. The fracture occurred from layer-to-layer delamination at the follow legs, which could be a reason for the fracture location not matching the FEA prediction.

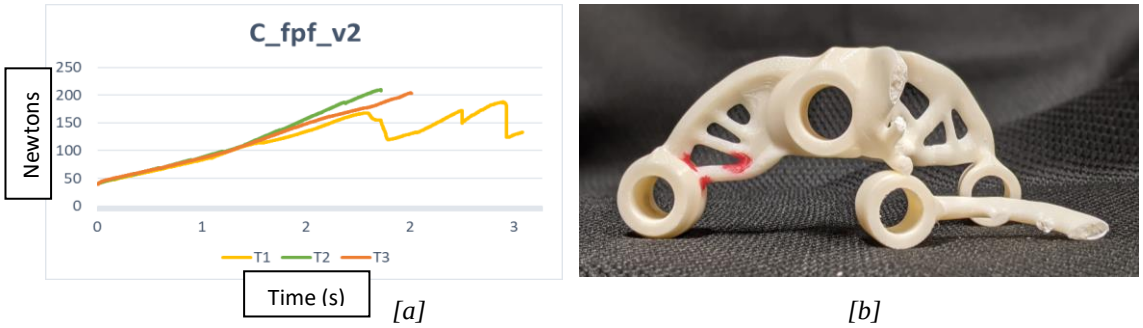

Figure 19: *C_fpf_v2 results [a] and fractures [b]*

Bk_fpx was the strongest part, failure summary below. This sample experienced failure at multiple points and was the strongest sample. Note: Three samples were run but graph only shows one line because test data was corrupted during graphing.

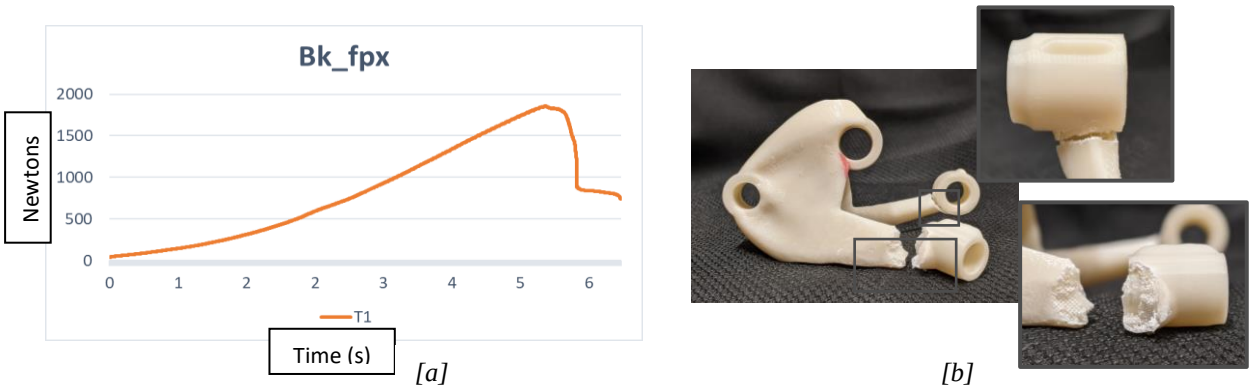

Figure 20: *Bk_fpx results [a] and fractures [b]*

Table 6: Fracture Testing End Results

Sample	Max Tensile (MPa)	Weight (g)	Ult. Force (N)	Ratio (N/g)	Elongation (mm)
C_fpf_Robust	83.7	50.3	835.7	16.6	11.5
	83.6	50.5	836.5	16.6	9.2
	88.0	51.0	879.6	17.2	14.3
Avg.	85.1	50.6	850.6	16.8	11.7
C_fpf_Light	20.9	37.3	209.5	5.6	4.5
	18.8	37.0	187.7	5.1	7.1
	20.4	36.8	203.9	5.5	5.0
Avg.	20.0	37.0	200.3	5.4	5.5
Bk_fpx	**185.9**	**62.6**	**1859.1**	**29.7**	**12.0**
	145.8	63.7	1458.4	22.9	16.1
	120.2	63.2	1201.8	19.0	9.7
Avg.	150.6	63.2	1506.4	23.9	12.6

Conclusion

After testing four different designs with three samples of each, the block based over_pin design approach, Bk_fpx, was able to withstand the most load (1859 N) compared to all of the other designs. Bk_fpx also had the best specific strength, otherwise known as its strength to weight ratio (29.7) and was the second cheapest option with a cost of $160 using ABS model and F123 QSR soluble support material.

It is important to mention that each of the designs provided consistent results across their replicas, however Bk_fpx had the biggest difference in results. The reason for this might be attributed to some material having to be manually shaven off as the design couldn't fit on the testing fixture. This issue derived from the pin connection configuration of the sample, where the over_pivot approach was not considered when designing the fixture. In addition, Bk_fpx is 62.6 grams, 3 grams heavier than the original design but it is almost four times stronger. This design can still be optimized to further reduce weight and to re-distribute the amount of material in some areas where no stress concentration was shown on the FEA nor the real test. This, while also reinforcing the failure points.

Optimization could also be done regarding material support and printing settings. As this could help to reduce amount of material used and consequently in less time and cost. This since printing settings used were the default ones provided by GrabCAD.

In terms of strength, cost, weight, design approach, orientation and room for improvement, Bk_fpx is the best approach for a bell crank AM using FDM. This approach could be modified

and tailored towards other AM technologies such as EBM (Electron Beam Melting) or LPBF (Laser Powder Bed Fusion).

Further Development/Future Work

After finishing the testing phase, Bk_fpx and C_fpf_v2 were additively manufactured once more, this time using the SLM approach. Again, all material and printing services were provided by the W.M. Keck Center for 3D Innovation. For this print, Aluminum F357 was used since this material is considered to be a lightweight metal and therefore adheres to the aircraft reduced weight goal[12]. The main purpose of this phase was to introduce SLM's LPBF as a rapid prototyping method. SLM prototypes were fabricated to evaluate resolution, success rate, and effectiveness of build. To preserve resources, these samples were scaled down in size. This method was also chosen due to its capability of producing high density results which makes the parts exhibit similar mechanical properties as their traditionally manufactured counterparts[13], [14]. Future work will consist of replicating the FDM model fracture testing onto the SLM pieces while also following military standards and constraints not previously specified with the initial portion of the experiment.

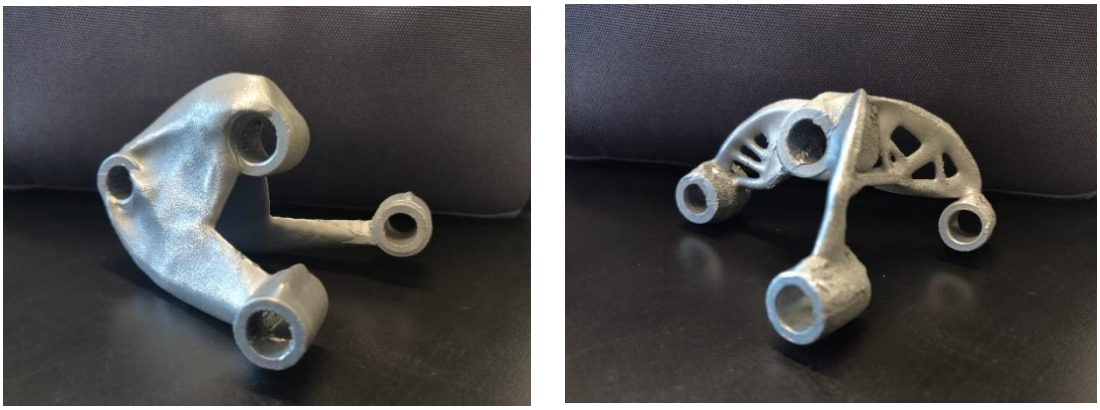

[a] *[b]*

Figure 21: *Aluminum Bk_fpx [a] and C_fpf_Light [b]*

Acknowledgments

The work was sponsored by the Aire Force Research Laboratory under contract W911NF-16-2-0019. We want to thank the following undergraduate students: Sol Barraza (e-mail: sabarraza2@miners.utep.edu), Carlos Rodriguez (e-mail: carodriguez30@miners.utep.edu), Julio Diaz (e-mail: jcdiaz6@miners.utep.edu), and Alejandro Hernandez (email: ajhernandez24@miners.utep.edu) from the University of Texas at El Paso under the mentorship of Dr. Francisco Medina from the W.M. Keck Center for 3D Innovation.

Bibliography

[1] C. Lindemann, U. Jahnke, M. Moi, and R. Koch, “Analyzing Product Lifecycle Costs for a Better Understanding of Cost Drivers in,” p. 12.

[2] T. C. Kros, “Modernization Through Spares : an analysis of implementation at the U.S. Army Aviation and Missile Command,” p. 102.

[3] B. Blakey-Milner et al., “Metal additive manufacturing in aerospace: A review,” Mater. Des., vol. 209, p. 110008, Nov. 2021, doi: 10.1016/j.matdes.2021.110008.

[4] G. Gong et al., “Research status of laser additive manufacturing for metal: a review,” J. Mater. Res. Technol., vol. 15, pp. 855–884, Nov. 2021, doi: 10.1016/j.jmrt.2021.08.050.

[5] T. Y. Pang and M. Fard, “Reverse Engineering and Topology Optimization for Weight-Reduction of a Bell-Crank,” Appl. Sci., vol. 10, no. 23, Art. no. 23, Jan. 2020, doi: 10.3390/app10238568.

[6] B. Aman, “Generative Design for Performance Enhancement, Weight Reduction, and its Industrial Implications,” p. 21.

[7] S. Raut, V. S. Jatti, N. K. Khedkar, and T. P. Singh, “Investigation of the Effect of Built Orientation on Mechanical Properties and Total Cost of FDM Parts,” Procedia Mater. Sci., vol. 6, pp. 1625–1630, Jan. 2014, doi: 10.1016/j.mspro.2014.07.146.

[8] R. H. Hambali, H. K. Celik, P. C. Smith, A. E. W. Rennie, and M. Ucar, “Effect of Build Orientation on FDM Parts: A Case Study for Validation of Deformation Behaviour by FEA,” p. 6, 2010.

[9] M. S. Srinidhi, R. Soundararajan, K. S. Satishkumar, and S. Suresh, “Enhancing the FDM infill pattern outcomes of mechanical behavior for as-built and annealed PETG and CFPETG composites parts,” Mater. Today Proc., vol. 45, pp. 7208–7212, Jan. 2021, doi: 10.1016/j.matpr.2021.02.417.

[10] K. Arunprasath et al., “Dynamic mechanical analysis performance of pure 3D printed polylactic acid (PLA) and acrylonitrile butadiene styrene (ABS),” Mater. Today Proc., Sep. 2021, doi: 10.1016/j.matpr.2021.09.113.

[11] K. G. J. Christiyan, U. Chandrasekhar, and K. Venkateswarlu, “A study on the influence of process parameters on the Mechanical Properties of 3D printed ABS composite,” IOP Conf. Ser. Mater. Sci. Eng., vol. 114, p. 012109, Feb. 2016, doi: 10.1088/1757-899X/114/1/012109.

[12] “AM behind the scenes | Elsevier Enhanced Reader.” https://reader.elsevier.com/reader/sd/pii/S0026065717301170?token=2D3D28BB23308027E0FD1D0C7E5165747DE7D6E324AC3102A4FD137FBF69794A8A

C82C127C4E574452A7AB1C0157655E&originRegion=us-east-1&originCreation=20211005184409 (accessed Oct. 05, 2021).

[13] D. Gu, F. Chang, and D. Dai, “Selective Laser Melting Additive Manufacturing of Novel Aluminum Based Composites With Multiple Reinforcing Phases,” J. Manuf. Sci. Eng., vol. 137, no. 2, Apr. 2015, doi: 10.1115/1.4028925.

[14] K. A. Mumtaz, P. Erasenthiran, and N. Hopkinson, “High density selective laser melting of Waspaloy®,” J. Mater. Process. Technol., vol. 195, no. 1, pp. 77–87, Jan. 2008, doi: 10.1016/j.jmatprotec.2007.04.117.